Selective Functionalization of 3D Matrices Via Multiphoton Grafting and Subsequent Click Chemistry

Aleksandr Ovsianikov, Zhiquan Li, Jan Torgersen, Jürgen Stampfl, and Robert Liska**

Grafting is a popular approach for adjusting the properties and functionalization of various surfaces. Conventional photoinduced grafting has been utilized on flat surfaces, porous monoliths, and hydrogels. By masking or illuminating only a portion of the sample, a certain degree of spatial and temporal control is possible, but the ability to use grafting to pattern in 3D is limited. Here, the laser-induced photolysis of an aromatic azide compound is employed for true 3D photografting within a poly(ethylene glycol) (PEG)-based matrix. Since the multiphoton interaction occurs only in a confined area within the laser focal spot, the localized immobilization of a selected molecule with high spatial resolution in 3D is possible. In contrast to the widely utilized chain-growth polymerization-based grafting, the approach is characterized by a single-molecule insertion mechanism. Successful binding of the fluorophore is confirmed by laser scanning microscopy. To test for the presence of latent azides and to determine the suitability for additional postmodification with arbitrary functional groups, the sample is further subjected to copper-catalyzed alkyne click-reaction conditions. The described 3D photografting method is simple, highly efficient, and universal. The presented results demonstrate the great potential of multiphoton-induced grafting for 3D site-specific functionalization.

1. Introduction

Molecular grafting provides a means for tailoring the physicochemical properties of surfaces. Its current applications range from electronic, such as solar cells and sensors,[1] to biomedical engineering.[2,3] Photoinduced grafting provides the additional advantages of spatial and temporal control of the process. Apart from producing micropatterns, the surface density of the covalently immobilized molecules can be adjusted by tuning the exposure dose.[4] Furthermore, using molecules that respond to different wavelengths, it is possible to pattern multiple species onto the same substrate sequentially.[5]

One of the most interesting research applications of photografting is the modulation of properties of cell-culture substrates. In natural tissues, cells recognize and attach to specific amino acid sequences in extracellular-matrix (ECM) protein molecules via integrins.[6] The importance of incorporating biomimetic signals within artificial matrices has long been recognized. The main idea is to mimic the ECM components and study cell behavior – such as adhesion, spreading, migration, or differentiation – in response to the grafted molecules and patterns.[4] Clemens et al. reported on the synthesis and photoimmobilization of bioactive laminin fragments.[7] Laminin-functionalized substrates produced by UV irradiation through a photomask were shown to induce pattern-guided neuronal cell adhesion. Fibroblast adhesion onto the substrate can be modulated by immobilized RGD-peptide at different densities; as a result, the shape and the distribution of the adhering cells can be controlled.[4]

Due to technical limitations, most studies using photografting have been conducted on flat surfaces. The possibility of producing volumetric patterns decorated with biomolecules is very appealing for tissue engineering, as it brings the in vitro model much closer to the real 3D appearance of the natural ECM. By combining conventional lithographic methods with hydrogels to produce cell-adhesive channel-like patterns, a certain degree of "three-dimensionality" for cell-guiding applications has been approached.[8] True 3D grafting has been recently achieved using multiphoton excited photopatterning of hydrogels by Hahn et al.[9] In their work, immobilization of functional acrylate moieties was achieved by means of photoinitiator-mediated copolymerization with acrylate groups of the hydrogel matrix (not consumed during the initial UV polymerization). The same group later demonstrated, by attaching integrin ligands and signaling factors within an otherwise biologically passive hydrogel, that tubulogenesis can be accelerated corresponding to the upregulation of angiogenic genes within endothelial cells in 3D.[10]

Another emerging application of photografting is the functionalization of sensors employing specific molecular interactions. Sensor molecules are immobilized in order to create recognition sites for analyte molecules. It was reported that protein receptors can be grafted photochemically onto the surface of a germanium crystal within a Fourier-transform infrared (FTIR)

Dr. A. Ovsianikov, J. Torgersen, Prof. J. Stampfl
Vienna University of Technology
Institute of Materials Science and Technology
Favoritenstrasse 9-11, 1040 Vienna, Austria
E-mail: A.Ovsianikov@gmail.com
Z. Li, Prof. R. Liska
Vienna University of Technology
Institute of Applied Synthetic Chemistry
Getreidemarkt 9, 1060 Vienna, Austria
E-mail: robert.liska@tuwien.ac.at

DOI: 10.1002/adfm.201200419

spectroscopy detection system.[11] The possibility to produce localized recognition sites would strongly enhance sensing capabilities, especially in microfluidic sensors. An automated microcontact printing can be used for this purpose.[12] In this case, however, an additional assembly step is required in order to seal the channels. Sebra et al. have described controlled photografting of pH sensitive molecules by using a living radical polymerization technique.[13] The pH-sensitive surfaces produced this way are readily integrated onto a fully polymeric microfluidic device.

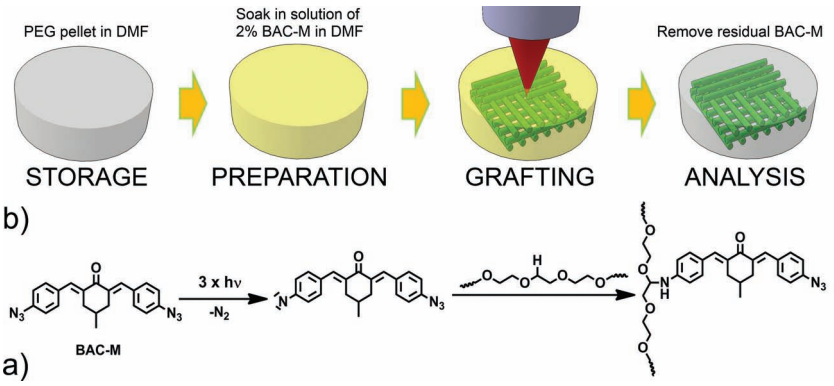

Figure 1. Schematic representation of the grafting process induced by multiphoton absorption: a) photolysis of aryl azide (BAC-M) followed by insertion reactions within the PEG sample and b) sample processing and multiphoton absorption induced grafting procedure.

Multiphoton photografting is potentially capable of immobilizing different molecules at defined locations. Since multiphoton reactions occur only in a confined area within the focal spot, more accurate functionalization can be obtained with higher resolution in a 3D volume. A closely related technique – two-photon polymerization – is already well-established in the field of direct laser writing.[14–17] It is an additive approach, most often relying on the highly efficient chain-growth polymerization chemistry. Furthermore, the selective functionalization was performed by writing 3D structures out of acrylates and methacrylates, consecutively. Post-modification of acrylate-based regions allows selective functionalization, such as metallization.[18] Another related technique – "two-photon uncaging" – utilizes cleavage of photolabile protecting groups in order to liberate useful functionalities in a localized fashion.[19–21] This subtractive approach is potentially more precise since the photolabile molecules are immobilized and thus cannot diffuse. Partly for the same reason, the involved chemistry is rather inefficient, which limits the applicability of the method despite the well-established chemistry.

Herein, we present our recent results on multiphoton-induced photografting with a reactive aromatic azide compound onto a highly permeable poly(ethylene glycol) (PEG)-based matrix. The utilized chemistry involves a single-molecule insertion mechanism, which represents a compromise between the two above-mentioned techniques, since it is potentially: i) more efficient, but less precise than uncaging; and, ii) more precise, but less efficient than chain-growth mechanisms. It is demonstrated that the patterning is possible within a large working parameter window, offered by the experimental setup. Multiphoton-induced grafting at a scanning speed of over 550 mm s^{-1} and with resolution down to 4 μm within the 3D matrix is reported. The produced patterns are further functionalized by means of a click reaction. The developed 3D site-specific functionalization method is simple and versatile; it has potential applications in microarray-based proteome analysis, studies of cell-surface interactions, sensing applications, and drug screening.

2. Results and Discussion

To demonstrate the utility of the new multiphoton grafting method, 2,6-bis(4-azidobenzylidene)-4-methylcyclohexanone (BAC-M) was selected as a suitable chromophore. The selection criteria for highly active molecules follow the principles well known from two-photon polymerization. These include planar π-conjugated systems containing strong donor and/or acceptor groups.[16,22,23] Our recent studies on multiphoton absorption by BAC-M at around 800 nm confirmed a high three-photon absorption cross section of 1.19×10^{-78} (cm^6 s^2).[24]

The mechanism of the multiphoton grafting process could be expected to follow the single photon grafting principle.[25] The focused laser beam interacts with the chromophore (**BAC-M**) via three-photon absorption (**Figure 1**a). Photolysis of the azide causes the dissociation of the N–N bond from the excited singlet state, followed by the generation of nitrogen and highly reactive electron-deficient nitrene species.[26] The short-lived nitrene intermediate is directly immobilized on the PEG-network by insertion into a C–H bond. This single-step process is universal, since it is applicable to a wide variety of matrices containing C–H or N–H bonds. In contrast to the more widely utilized chain-growth polymerization-based grafting, the presented approach is characterized by a single-molecule insertion mechanism. Since the multiphoton interaction is highly localized, the process of BAC-M immobilization on the PEG matrix is restricted to a limited volume. By moving the laser focus within the sample, 3D patterns of immobilized molecules can be "recorded" (Figure 1b). After grafting, either one or both azide groups can be covalently linked to the matrix. Both grafting products contain the ketocyanine chromophore, which exhibits strong fluorescence.[27] Therefore, grafted patterns can be directly observed via laser-scanning microscopy (LSM).

Figure 2a shows an array of squares produced at different laser power and scanning speed parameters. The BAC-M is found to have a large processing window from 30 mW to over 450 mW for laser power range at scanning speeds from 5 to over 550 mm s^{-1}. No patterns are observed at 20 mW and below, while the top laser power of 450 mW and speed of 550 mm s^{-1} are the limits of the current experimental setup. Despite the facts that the single-molecule insertion mechanism is much less efficient than the chain-growth polymerization, and that the three-photon absorption process is involved, the achieved scanning speed exceeds those reported for the two-photon polymerization process. These results also demonstrate the exposure dose-dependent fluorescence intensity, i.e., the fluorescent molecule immobilization density, of the multiphoton-induced grafting process.

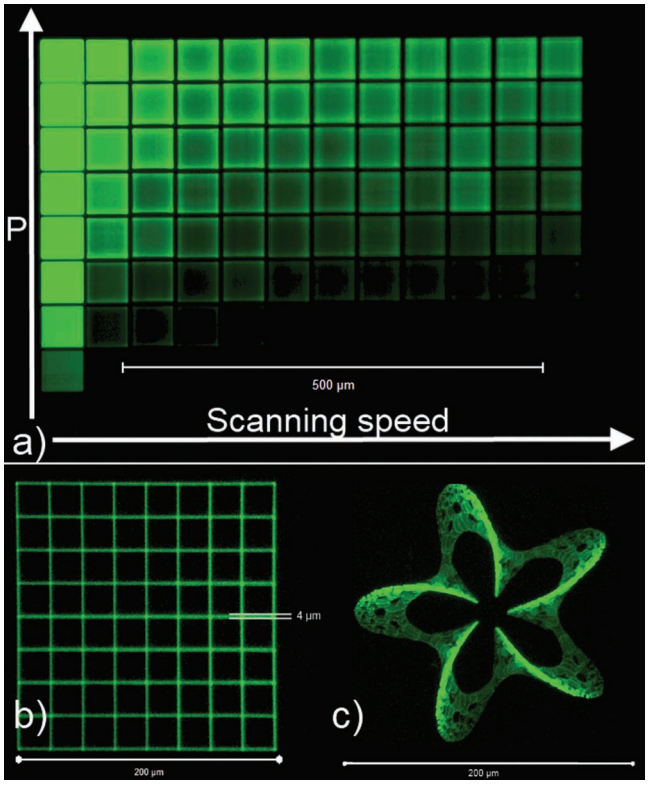

Figure 2. Patterns obtained by multiphoton induced photografting: a) an array of squares produced at different laser power (100–30 mW; step = –10 mW) and scanning velocity (5–555 mm s^{-1}; step = +50 mm s^{-1}) parameters; b) grid exhibiting the lateral resolution of around 4 µm; and c) complex 3D pattern – Echinodermania.[28] The scale bars represent 500, 200, and 200 µm in a, b, and c, respectively.

The 3D grid pattern produced by means of a single scan (450 mW, 5 mm s^{-1}) allows determination of the spatial resolution of the developed photografting process (Figure 2b). By using a conventional 20× microscope objective to focus the laser beam into the sample, lateral and vertical resolutions of around 4 and 17 µm are achieved, respectively. High spatial resolution of multiphoton grafting allows the realization of such complex 3D patterns as Echinodermania (Figure 2c; see the Supporting Information for a complete 3D stack).[28] The use of immersion oil optics and shorter wavelength lasers will potentially allow even higher resolution due to tighter focusing and a further reduction of the light–material interaction volume.[29]

There are two different pathways for the introduction of functional groups. One method is to functionalize the aromatic azide prior to the photografting. This approach involves the synthesis of specific compounds for every application. A second, and much more universal, approach, is the post-modification of the already grafted azide. The produced patterns contain various reactive groups allowing subsequent post-modification. The keto group can be modified with substituted hydrazines and the double bonds can be used in the thiol–ene click reaction. It has to be noted that the residual double bonds from the PEG matrix used would be involved with the latter type of reaction and thus have to be deactivated before the grafting procedure (e.g., by thiol–ene). Nevertheless, in other matrix materials, this concept could be applied without any disadvantages. The most straightforward procedure is to use the remaining azide groups for the subsequent functionalization via the azide–yne click reaction.[30] As a model precursor for the click reaction, a Br-containing alkyne **1** was synthesized via alkylation of a phenol derivative with 3-bromoprop-1-yne (**Figure 3**a). The produced compound was immobilized to the patterned area by means of a copper(I)-catalyzed azide–alkyne cycloaddition (CuAAC) reaction in a tetrahydrofuran (THF) solution (Figure 3b). The successful immobilization was verified by EDX screening of the Br content on the grafted area and also by model reaction (see the Supporting Information). Since EDX is only capable of analyzing a thin layer of material, a larger and denser grafted pattern was produced on and a few micrometers into the surface of the sample for this purpose. After post-modification with the Br-containing alkyne **1**, the line scan through the functionalized area yielded a Br distribution profile reproducing the shape of the photografted pattern (Figure 3c). The quantitative evaluation of the Br content was performed by EDX scanning of the equal grafted and control areas. The weight content of Br, calculated relative to the primary elements of the sample (C and O), was 5 ‰ on the grafted area and 0.5 ‰ outside the pattern. Despite the low relative concentration of Br on the sample, the tenfold increase of its content indicates the selective functionalization of the grafted area by means of the click reaction.

3. Conclusions

In conclusion, we have developed a versatile and straightforward photografting method based on laser photolysis of an aromatic

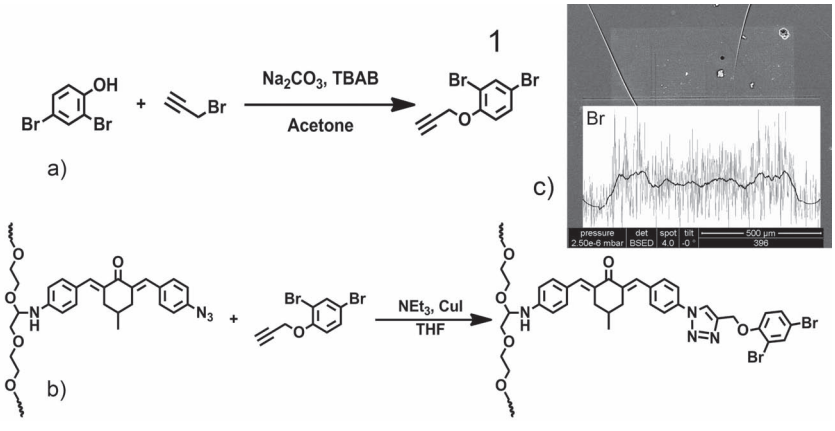

Figure 3. Functionalization of photografted patterns via click chemistry: a) synthesis of Br-containing precursor 1; b) immobilization of the precursor via a CuAAC click reaction; and c) energy-dispersive X-ray spectroscopy (EDX) analysis of sample photografted and subsequently functionalized with Br-containing compound. A line scan through the photografted pattern (light area in the SEM image) shows the distribution of Br.

azide compound. Since multiphoton-induced reactions occur in a confined area within the laser focal spot, accurate functionalization with high spatial resolution in 3D is possible. A PEG matrix was used as a model substrate for localized grafting. However, the presented results are applicable to a wide variety of matrices containing C–H or N–H bonds. A highly selective molecule immobilization with the lateral resolution down to 4 μm in 3D was achieved.

To confirm that arbitrary molecules can be immobilized within a 3D volume, patterns produced by photografting were further functionalized by means of copper(I)-catalyzed azide–alkyne cycloaddition (CuAAC). Due to the distinct features of the click reactions, the application range of "functionalization" can be largely extended by utilizing various alkyne derivatives. To the best of our knowledge, this is the first report utilizing aromatic azide compounds for multiphoton-induced grafting and their further functionalization via a click reaction. The achieved feature size is substantially smaller than the dimensions of most mammalian cells, while the patterned volume is large enough for studies of single-cell attachment and migration.

Along with high scanning speed of over 550 mm s^{-1}, demonstrated here, the presented results indicate the great potential of the developed 3D site-specific functionalization method for possible applications in microarray-based proteome analysis, studies of cell-surface interactions, sensing applications, and drug screening.

4. Experimental Section

Laser Grafting via Multiphoton Absorption: The samples were prepared from poly(ethylene glycol) diacrylate (PEGda, $\overline{M}_n$ 700, Sigma Aldrich) diluted with DMF (dimethylformamide), with an addition of 1 wt -% of the photoinitiator Irgacure 2959 (Ciba SC). The resulting formulation was photopolymerized with UV light for 5 min (Intelliray 600) in silicone molds (diameter 6 mm; thickness 1 mm). The photopolymerized material pellets were soaked in 50% EtOH solution for at least 1 week, with the solvent being exchanged on a regular basis, in order to remove residual monomer and photoinitiator. Next, the EtOH was replaced with DMF and the samples were stored until use. For laser photografting, the samples were immersed into the 2 wt-% solution of BAC-M in DMF (Figure 1b). A Ti:sapphire femtosecond laser (High Q, Femtotrain), emitting pulses with duration of 80 fs at a 73 MHz repetition rate around 793nm is used for laser grafting. The laser beam was focused with a 20× microscope objective (Zeiss, NA = 0.8) into the sample. An acousto-optical modulator was used for fast switching of the laser beam and for adjusting its intensity. The laser power was measured before the objective. The patterns were obtained by scanning the focused laser beam within the sample with the galvo-scanner (HurryScan, ScanLab). In addition, the sample was mounted on an assembly of three linear translation stages for complete 3D movement. The grafted patterns were produced by a set of adjacent line scans: Figure 2a and c at a distance of 0.5 μm; and, Figure 2b at a distance of 25 μm. While the pattern in Figure 2b is composed of a single layer, a step of 5 μm was used in the vertical direction was used otherwise. A control experiment, involving the laser operated in CW mode, confirmed that no patterns can be produced at the average laser powers utilized for photografting in a mode-locked regime.

After the grafting procedure, the samples were placed in DMF in order to remove the residual BAC-M. Rapid decoloration of the pellet indicated the successful removal of possible residuals form the sample. The fluorescence of the patterned samples was analyzed by laser scanning microscopy (LSM700, ZEN software, Carl-Zeiss), at the excitation wavelength of 488nm.

Materials: All reagents for the synthesis of precursor 1 and the model CuAAC reaction were purchased from Sigma-Aldrich, Fluka, and ABCR and used without further purification. The solvents were dried and purified by standard laboratory methods or were dried over Al_2O_3 cartridges. Petroleum ether refers to the fraction boiling in the range 40–60 °C. Column chromatography was performed with conventional techniques on VWR silica gel 60 (0.040–0.063 mm particle size). Aluminium-backed silica gel plates were used for TLC analysis.

Characterization: ^{1}H NMR (200 MHz) and ^{13}C NMR (50 MHz) spectra were measured with a BRUKER ACE 200 FT-NMR-spectrometer. The chemical shift (s = singlet, bs = broad singlet, d = doublet, t = triplet, m = multiplet) is stated in ppm using the nondeuterated solvent as internal standard. Solvents with a grade of deuteration of at least 99.5% were used. GC-MS runs were performed on a Thermo Scientific DSQ II using a BGB 5 column (l = 30 m, d = 0.32 mm, 1.0 μm film; achiral).

Synthesis of 2,4-Dibromo-1-(prop-2-ynyloxy)benzene (1): For the synthesis of **1**, anhydrous K_2CO_3 (1.06 g, 10 mmol) was added to a solution of 2,4-dibromophenol (2.51 g, 10 mmol), 3-bromoprop-1-yne (1.79 g, 15 mmol) and tetra-*n*-butylammonium bromide (50 mg, 0.15 mmol) in acetone (50 mL). The suspension was stirred at 60 °C under an argon atmosphere until the 2,4-dibromophenol was completely consumed (GC-MS analysis). The mixture was filtered off, the solid residue was washed with ethyl acetate and the volatile compounds were removed in vacuum. The crude product was dissolved in ethyl acetate and washed with water and brine. The organic layer was dried over sodium sulfate, filtered and concentrated. The purification by column chromatography (petroleum ether: ethyl acetate = 8:1) yielded 2.67 g (92%) of product **1** as a light yellow solid with a melting point at 69–71 °C; ^{1}H NMR (200MHz,DMSO-d_6) δ = 7.80 (d, J = 2.2 Hz, 1 H), 7.56 (dd, J = 2.2, 8.9 Hz, 1 H), 7.14 (d, J = 9.0 Hz, 1 H), 4.91 (d, J = 2.2 Hz, 2 H), 3.64 (t, J = 2.1 Hz, 1 H). ^{13}C NMR (50MHz,DMSO-d_6) δ = 153.0, 134.8, 131.4, 115.9, 113.0, 112.2, 79.1, 78.3, 56.7. GC-MS: (m/z) 63.11, 74.07, 102.13, 130.12, 182.01, 211.05, 222.95, 250.95, 260.95, 289.91, 291.91.

Functionalization of the Grafted Area by Means of a Click Reaction: 20 mg (0.068 mmol) of 2,4-dibromo-1-(prop-2-ynyloxy)benzene were dissolved in 3 mL degassed THF in a brown glass vial. To the solution, laser-grafted pellets, 10 mg (0.052 mmol) of CuI and 0.1 mL degassed triethylamine were added. The vial was placed on a rotation mixer after being sealed and the reaction was carried out at room temperature under argon for 12 h. Afterwards, the pellet was removed, washed several times with fresh DMF to remove residual 2,4-dibromo-1-(prop-2-ynyloxy) benzene and dried under vacuum. The successful immobilization of the precursor was verified by measuring the content of Br on the produced samples by means of energy-dispersive X-ray spectroscopy (EDX). The sample was sputter-coated with a 20 nm Pd/Au layer prior to the analysis with a scanning electron microscopy (Quanta FEG).

Supporting Information

Supporting Information is available from the Wiley Online Library or from the author.

Acknowledgements

The financial support of the Austrian Research Agency FFG under contract 819718 (ISOTEC), the Chinese Scholarship Council, and the ESF-P2M program is gratefully acknowledged. This project is partially funded by the EU Framework 7 Programme, contract no. 260043 (PHOCAM). We would like to thank Dipl.-Ing. Enrico Dall'Ara for his technical assistance with the LSM.

Received: February 10, 2012
Published online: May 21, 2012

[1] G. Ashkenasy, D. Cahen, R. Cohen, A. Shanzer, A. Vilan, *Acc. Chem. Res.* **2002**, *35*, 121–128.
[2] I. Bisson, M. Kosinski, S. Ruault, B. Gupta, J. Hilborn, F. Wurm, P. Frey, *Biomaterials* **2002**, *23*, 3149–3158.
[3] S. Jaumotte-Thelen, I. Dozot-Dupont, J. Marchand-Brynaert, Y.-J. Schneider, *J. Biomed. Mater. Res.* **1996**, *32*, 569–582.
[4] C. B. Herbert, T. L. McLernon, C. L. Hypolite, D. N. Adams, L. Pikus, C.-C. Huang, G. B. Fields, P. C. Letourneau, M. D. Distefano, W.-S. Hu, *Chem. Biol.* **1997**, *4*, 731–737.
[5] M. A. Holden, P. S. Cremer, *J. Am. Chem. Soc.* **2003**, *125*, 8074–8075.
[6] E. Alsberg, H. A. von Recum, M. J. Mahoney, *Expert Opin. Biol. Ther.* **2010**, *6*, 847–866.
[7] J.-F. Clemence, J. P. Ranieri, P. Aebischer, H. Sigrist, *Bioconjugate Chem.* **1995**, *6*, 411–417.
[8] Y. Luo, M. S. Shoichet, *Nat. Mater.* **2004**, *3*, 249–253.
[9] M. S. Hahn, J. S. Miller, J. L. West, *Adv. Mater.* **2006**, *18*, 2679–2684.
[10] J. E. Leslie-Barbick, C. Shen, C. Chen, J. L. West, *Tissue Eng. Part A* **2010**.
[11] J. Conti, A. Goldsztein, E. Gosselin, A. Brans, M. Voue, J. De Coninck, F. Homble, E. Goormaghtigh, J. Marchand-Brynaert, *J. Colloid Interface Sci.* **2009**, *332*, 408–415.
[12] E. Bou Chakra, B. Hannes, J. Vieillard, C. D. Mansfield, R. Mazurczyk, A. Bouchard, J. Potempa, S. Krawczyk, M. Cabrera, *Sens. Actuators, B* **2009**, *140*, 278–286.
[13] R. P. Sebra, A. M. Kasko, K. S. Anseth, C. N. Bowman, *Sens. Actuators: B* **2006**, *119*, 127–134.
[14] A. Ovsianikov, V. Mironov, J. Stampfl, R. Liska, *Expert Rev. Med. Devices* **2012**.
[15] S. Maruo, J. T. Fourkas, *Laser Photon. Rev.* **2008**, *2*, 100–111.
[16] M. Rumi, S. Barlow, J. Wang, J. W. Perry, S. R. Marder, in *Photoresponsive Polymers* (Eds: S.R. Marder, K.-S. Lee), Springer, Berlin, Heidelberg **2008**, 1–95.
[17] *3D Laser Microfabrication: Principles and Applications*, (Eds: H. Misawa, S. Juodkazis) Wiley-VCH, Weinheim **2006**.
[18] R. A. Farrer, C. N. LaFratta, L. Li, J. Praino, M. J. Naughton, B. E. A. Saleh, M. C. Teich, J. T. Fourkas, *J. Am. Chem. Soc.* **2006**, *128*, 1796–1797.
[19] T. Furuta, *Proc. Natl. Acad. Sci. USA* **1999**, *96*, 1193–1200.
[20] E. B. Brown, J. B. Shear, S. R. Adams, R. Y. Tsien, W. W. Webb, *Biophys. J.* **1999**, *76*, 489–499.
[21] R. G. Wylie, S. Ahsan, Y. Aizawa, K. L. Maxwell, C. M. Morshead, M. S. Shoichet, *Nat. Mater.* **2011**, *10*, 799–806.
[22] B. H. Cumpston, S. P. Ananthavel, S. Barlow, D. L. Dyer, J. E. Ehrlich, L. L. Erskine, A. A. Heikal, S. M. Kuebler, I.-Y. S. Lee, D. McCord-Maughon, J. Qin, H. Rockel, M. Rumi, X.-L. Wu, S. R. Marder, J. W. Perry, *Nature* **1999**, *398*, 51–54.
[23] N. Pucher, A. Rosspeintner, V. Satzinger, V. Schmidt, G. Gescheidt, J. Stampfl, R. Liska, *Macromolecules* **2009**, *42*, 6519–6528.
[24] A. Ovsianikov, Z. Li, A. Ajami, J. Torgersen, W. Husinsky, J. Stampfl, R. Liska, *Applied Physics A* **2012**,DOI: 10.1007/s00339-012-6964-9.
[25] G. B. Schuster, M. S. Platz, in *Advances in Photochemistry*, (Eds: D. H. Volman, G. S. Hammond, D. C. Neckers), John Wiley & Sons, Inc., Hoboken, NJ **1992**, 69–143.
[26] R. Pinard, J. E. Heckman, J. M. Burke, *J. Mol. Biol.* **1999**, *287*, 239–251.
[27] J. M. Eisenhart, A. B. Ellis, *J. Org. Chem.* **1985**, *50*, 4108–4113.
[28] G. Hart, Rapid Prototyping Models, http://www.georgehart.com/rp/rp.html (January 2012).
[29] W. Haske, V. W. Chen, J. M. Hales, W. Dong, S. Barlow, S. R. Marder, J. W. Perry, *Opt. Express* **2007**, *15*, 3426.
[30] C. W. Tornøe, C. Christensen, M. Meldal, *J. Org. Chem.* **2002**, *67*, 3057–3064.